Square to stripe transition and superlattice patterns in vertically oscillated granular layers

Hwa-Kyun Park*
Max-Planck Institut für Physik komplexer Systeme, Dresden 01187, Germany

Hie-Tae Moon
Department of Physics, Korea Advanced Institute of Science and Technology, Taejon 305-701, Korea
(Received 19 November 2001; published 22 May 2002)

We investigated the physical mechanism for the pattern transition from square lattice to stripes, which appears in vertically oscillating granular layers. We present a continuum model to show that the transition depends on the competition between inertial force and local saturation of transport. By introducing multiple free-flight times, this model further enables us to analyze the formation of superlattices as well as hexagonal lattices

DOI: 10.1103/PhysRevE.65.051310 PACS number(s): 45.70.Qj, 47.54.+r

Vertically oscillated granular layers exhibit various interesting patterns, such as subharmonic stripes, squares, hexagons, as well as localized structures called oscillons [1–7]. The control parameters are the driving frequency f and the dimensionless acceleration $\Gamma = 4\pi^2 f^2 A/g$, where g is the acceleration due to gravity and A is the amplitude of the vibrating surface. Increasing Γ with fixed f, flat states, subharmonic squares or stripes depending on f, subharmonic hexagons, and flat states appear in sequence.

These granular patterns have been studied using phenomenological models [8–15] and molecular dynamics simulations [16]. The studies show that transitions between granular patterns as Γ increases are related to the period doubling bifurcation [2,12]. But the bifurcation as a function of f, that is, the transition between squares and stripes, has not been well understood yet. There have been many models showing both squares and stripes [8,10,12,16] and it was suggested that the effective viscosity and the horizontal mobility resolve the transition [2,8,9]. Experiments also show that squares arise at large lateral transport while stripes form at small lateral transport [5]. However, there has been no explicit model for the square to stripe transition upon increasing frequency.

In this paper, we propose a continuum model that describes the transition between squares and stripes. We incorporate the lateral transfer and the local saturation mechanism into our model. The study shows that the ratio of these two competing processes depends on the frequency, which explains the dependence of the square-stripe transition on the drive frequency. In addition, considering multiple free-flight times, we study the hexagonal and superlattice patterns, which are observed in the granular system with multiple frequency forcing [7].

The granular patterns are similar to the Faraday waves in vibrated fluids [17], however, some differences exist.

(i) On each cycle, there is a free-flight time during which the granular layer loses contact with a bottom plate.

(ii) In general, macroscopic physical quantities for the granular material are not well defined. But Ref. [6] shows that a continuum description of the granular layer is valid for the square-stripe transition. Molecular simulation results [16] also suggest that granular continuum equations can be used as far as pattern formation of vertically oscillated granular media is concerned.

(iii) Granular material has an angle of repose, and shows both solidlike and liquidlike motions.

Considering (i) and (ii), a continuum equation is introduced with two steps: contact with the bottom plate, and free flight. It provides the two competing processes, diffusion during the contact and focusing effect during the free flight, which were suggested as mechanisms of subharmonic wave generation [9]. A hysteresis effect due to (iii), which accounts for the formation of the oscillon [9,10,12–15], is not considered here since it appears to be unrelated to the square-stripe transition [6].

At $t=0$, the layer collides with the bottom plate and the slope of granular layers begins to relax. From the collision, granular particles get kinetic energy and move randomly. The process can be described as diffusion, and the following equation is obtained for $0 \leqslant t < t_c$ during which granular layers have contact with the bottom plate

$$\rho_t = D\nabla^2 \rho. \tag{1}$$

We assume that the thickness h is a monotonic increasing function of the local density ρ, where ρ is a mass of granular material per unit area, and choose ρ as an order parameter.

At $t=t_c$, the layer loses contact with the bottom plate. During the free flight, the lateral transfer of grains induces the focusing of the sands, so that subharmonic excitation of the granular wave occurs. From continuity, the flux $\vec{j}$ and the velocities $\vec{v}$ of grains right after the takeoff from the bottom plate are given by

$$\begin{aligned} \vec{j}(\vec{x},t_c) &= -D\nabla\rho(\vec{x},t_c), \\ \vec{v}(\vec{x},t_c) &= \vec{j}(\vec{x},t_c)/\rho(\vec{x},t_c) = -D\nabla\rho(\vec{x},t_c)/\rho(\vec{x},t_c). \end{aligned} \tag{2}$$

*FAX: +49-351-871-1999; Email address: childend@complex.kaist.ac.kr

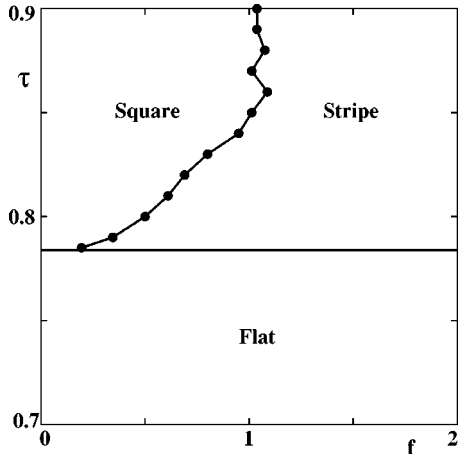

FIG. 1. Bifurcation diagram as a function of f and τ. $\alpha=0.015$, $D=0.17$,$l=10$.

This is indeed what was done by Cerda *et al.* [9], in which saturation of the flux is not considered, and only square patterns arise. Hence one may expect that the saturation is related to the formation of stripe patterns. Assuming that granular layers behave like fluid during the free flight, we adopt Navier-Stokes equations in two dimensions as a model of the the local saturation of flux as well as the transfer of particles and momentum.

During the interval $t_c \leqslant t < T$, where $T=1/f$ is the period of the driving force, we get

$$\rho_t + \nabla\cdot(\rho\vec{v}) = 0,$$

$$\vec{v}_t + \vec{v}\cdot\nabla\vec{v} = -\frac{1}{\rho}\nabla p. \tag{3}$$

Momentum is transferred through the transport of the granular particle, and inelastic collisions between the particles suppress the lateral motions. In general, these effects can be incorporated into the local stress tensor T_{ij}. Assuming that the suppression of the lateral motion is most important, the local stress tensor is approximated by $T_{ij} = -p\,\delta_{ij}$. When we consider the collision between granular particles, the relevant variable is a relative velocity rather than a velocity itself. A dimensional consideration leads to the following form of the pressure:

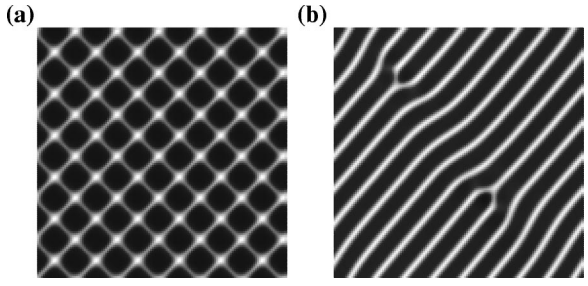

FIG. 2. Square and stripe patterns. White corresponds to the large ρ. $D=0.17$, $l=10$, $\alpha=0.015$, $\tau=0.85$. (a) $T=1.2$; (b) $T=0.7$.

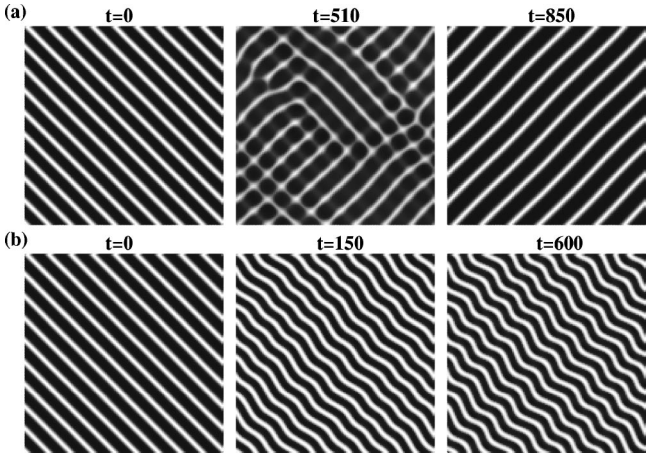

FIG. 3. Instabilities of stripes. $\alpha=0.015$, $D=0.17$, $l=10$. For $t<0$, $T=0.55$, and at $t=0$, $T=1/f$ is changed abruptly. (a) $T=0.85$ represents crossroll instability; (b) $T=0.30$ represents zigzag instability.

$$p = -\alpha\rho|\nabla\cdot\vec{v}|\nabla\cdot\vec{v}. \tag{4}$$

The pressure is high at the accumulation points where $\nabla\cdot\vec{v}<0$, and low at the dispersion points where $\nabla\cdot\vec{v}>0$. The pressure difference produces the force to suppress the focusing of sands. The parameters of Eqs. (1),(2), (3), and (4) are D, f, α, and $\tau = t_f/T = 1 - t_c/T$ where t_f is a free-flight time. In a real system, τ is determined mainly by Γ. D and α depend on layer depth, grain diameter, and restitution coefficient as well as Γ and f. We choose $\alpha=0.015$, $D=0.17$, and system size $l=10$.

Linear stability analysis for the rest state shows that the amplitude of the mode with wave number k is amplified by the Floquet multiplier $F(k)=(1-Dk^2\tau T)\exp[-Dk^2(1-\tau)T]$ on each cycle. At small τ, we get only flat states. As τ is increased beyond $\tau_c=0.782$, which is independent of D and T, minimum value of $F(k)$ becomes less than -1 and subharmonic standing waves arise. In this case, we obtain the dispersion relation, $f=D\tau(1-\tau)k^2$. Note that the value of τ_c does not depend on D, f, α, and l. The bifurcation diagram of Eqs. (1) and (3) as a function of f and τ is presented in Fig. 1; Fig. 2 describes typical patterns. With increasing f with fixed α and τ , one can see the square to stripe transition as in Figs. 2(a) and 2(b).

Increasing α with fixed f and τ also yields the square to stripe transition. In other words, the local saturation prefers stripe patterns. It is interesting to compare the results with the Faraday waves. In Faraday waves, squares are observed for small viscosities while stripes for large viscosities [17]. In this case viscosity represents the strength of local saturation that competes with the inertial force.

To understand the relation between the square-stripe transition and the drive frequency, let us write the equations in dimensionless forms. Naturally, we take $T=1/f$ as the time unit. For the length unit, we choose $\sqrt{D/f}$ that reflects the wavelength. Inserting $t=\hat{t}/f$, $\nabla=\hat{\nabla}/\sqrt{D/f}$, $v=\sqrt{Df}\hat{v}$, into Eq. (1), Eq. (3) with Eq. (4), and dropping the carets, we get for $0\leqslant t<1-\tau$,

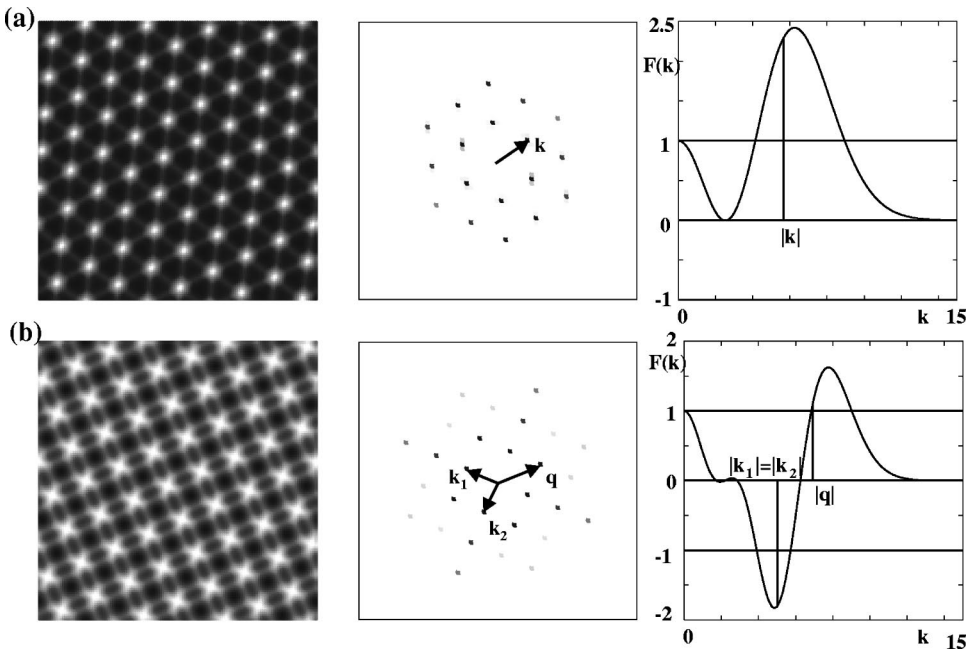

FIG. 4. Hexagon and superlattice patterns. Left: hexagonal and superlattice patterns. Middle: power spectra of the left image. Right: Floquet multiplier $F(k)$ vs k. $D=0.17$, $l=10$, $\alpha=0.015$. (a) $t_{c1}=0.28$, $t_{c2}=0.08$, $t_{f1}=0.84$, and $t_{f2}=1.02$. (b) $t_{c1}=0.08$, $t_{c2}=0.18$, $t_{c3}=0.31$, $t_{c4}=0.03$, $t_{f1}=0.72$, $t_{f2}=1.21$, $t_{f3}=2.00$, and $t_{f4}=0.15$.

$$\rho_t=\nabla^2\rho, \tag{5}$$

and for $1-\tau\leqslant t<1$,

$$\rho_t+\nabla\cdot(\rho\vec{v})=0,$$

$$\vec{v}_t+\vec{v}\cdot\nabla\vec{v}=\frac{R}{\rho}\nabla(\rho|\nabla\cdot\vec{v}|\nabla\cdot\vec{v}), \tag{6}$$

where R is defined as $f\alpha/D$.

Now we have two dimensionless parameters. One is $\tau=t_f/T$, the fraction of flight time for one period, and the other is $R=f\alpha/D$ in Eq. (6), which corresponds to the ratio of the force causing the local saturation to the inertial force. Note that R is proportional to the frequency f. It means that increase in f induces the strong local saturation compared to the lateral movement. Qualitatively, this can be explained as follows. Lateral movements are suppressed by the inelastic collisions that are reflected by pressure p in our model. When wavelengths are short, the velocity differences between the neighboring grains are large, so is pressure p obtained Eq. (4). Hence, for high frequencies, the collision is dominant and mobility is suppressed.

Experimentally, the dispersion relation has a kink structure, i.e., it takes a different form below and above $f=f_c$ [5,6,16]. For almost all conditions, the square-stripe transition occurs for $f<f_c$ [6]. In other words, only the dispersion relation for $f<f_c$ is relevant as far as the square-stripe transition is concerned. In this regime, earlier experiments [1,5] reported an exponent 2, however, a recent experiment [6] yielded a different exponent value of 1.3. In contrast, in our model, the dispersion relation $\lambda\sim(D/f)^{1/2}$ is obtained. This contradiction can be resolved by considering the frequency dependence of the diffusion coefficient D [9,15]. Considering the relation between viscous length and energy injection rates, for fixed Γ, D scales like $1/f^3$ in the small frequency regime [9,18]. With this, $\lambda\sim(1/f^2)$ is obtained and the parameter R that measures the ratio of the saturation of mobility to the inertial force is proportional to f^4. Also note that influences of Γ on D and α have not been considered. Dependence of the square to stripe transition frequency on τ in Fig. 1, in contrast to the experimental result [6], where the transition frequency depends only on the layer depth H, may be attributed to this. Nevertheless, for fixed Γ, the above conclusion that squares transit to stripes with increasing the drive frequency does not change.

Next we consider the instability of stripe patterns. With an abrupt change of the driving frequency f, we observe a crossroll and a zigzag instabilities. Figure 3(a) shows an example of the crossroll instability. The stripes are unstable to crossrolls on both the high and low k sides in our model. Figure 3(b) illustrates the increase in wave vector k due to the zigzag instability. In experiments and molecular dynamics simulations [19], the stripe patterns have the crossroll instability for decreasing k, and the skew-varicose instability for increasing k. The zigzag instability has not been observed in experiments. Refining the stress tensor and comparing the results with the instabilities in experiments will yield more insights about the interaction between granular particles.

As external forcing Γ is increased, the motions are repeated after two different flight times and contact times. This period doubling causes hexagonal patterns [2], and the mechanism is investigated theoretically [12]. Recently, it has been reported that multiple frequency forcing on the granular layer yields superlattice patterns [7]. Similar patterns have been studied in the Faraday waves [20], driven ferrofluid surfaces [21], nonlinear optics [22], the Turing patterns [23], and the Rayleigh-Benard convection [24]. As in the single frequency forcing [3], the important variable determining patterns are expected to be the free-flight times and contact times.

To study the hexagons and superlattice patterns, we introduce the multiple free-flight times $t_{f1},t_{f2},\ldots,t_{fn}$ and con-

tact times $t_{c1}, t_{c2}, \ldots, t_{cn}$. Let us apply Eq. (1) during t_{c1} and Eq. (3) during t_{f1}. After that, we apply again Eq. (1) during t_{c2}, Eq. (3) during t_{f2}, and so on. The case with $n=2$ reduces to the period doubling and hexagonal patterns are obtained.

Linear stability analysis shows that the amplitude of the mode with wave number k is amplified by the factor $F(k)=\Pi_{i=1}^{n}(1-Dk^2t_{fi})\exp(-Dk^2t_{ci})$ on each cycle. For the hexagonal patterns, as expected, $F(k)$ gives a harmonic mode as in Fig. 4(a). However, in general, $F(k)$ can yield instabilities with various wavelengths and, as a result, superlattice patterns can be formed. In Fig. 4(b), the modes with $\vec{k}_1$ and $\vec{k}_2$ are subharmonic and the mode $\vec{q}$ is harmonic. They satisfy the resonance condition $\vec{k}_1+\vec{k}_2+\vec{q}=0$. Evidently, there is a large freedom of choice for the values of t_{ci} and t_{fi}. Analyzing the characteristics of the superlattice patterns in these vast parameter spaces is a problem for future studies.

In conclusion, based on the mass and momentum conservation law, we presented the continuum model to explain the transition between squares and stripes in vertically oscillated granular layers. Patterns are selected by two competing nonlinear interactions, the inertial force and the local saturation due to the inelastic collisions between granular particles. With increasing drive frequency, the local saturation gets stronger compared to the inertial force effect, so that the square to stripe transition occurs. Introduction of multiple free-flight times and contact times yields hexagonal patterns and superlattice patterns.

We thank S.-O. Jeong, T.-W. Ko, and P.-J. Kim for useful discussions, M. Bäer for useful comments, and H.K. Pak and P. Umbanhowar for notifying us of their experimental results. This work was supported by the interdisciplinary research program of the KOSEF (Grant No. KRF-2000-015-DP0097).

[1] F. Melo, P. Umbanhowar, and H.L. Swinney, Phys. Rev. Lett. **72**, 172 (1994).
[2] F. Melo, P. Umbanhowar, and H.L. Swinney, Phys. Rev. Lett. **75**, 3838 (1995).
[3] F. Melo, P. Umbanhowar, and H.L. Swinney, Nature (London) **382**, 793 (1996).
[4] P. Umbanhowar, F. Melo, and H.L. Swinney, Physica A **249**, 1 (1998).
[5] T. Metcalf, J. Knight, and H. Jaeger, Physica A **236**, 202 (1997).
[6] P. Umbanhowar and H.L. Swinney, Physica A **288**, 344 (2000).
[7] H.S. Wi, K. Kim, H.K. Pak, J. Korean Phys. Soc. **38**, 573 (2001).
[8] T. Shinbrot, Nature (London) **389**, 574 (1997).
[9] E. Cerda, F. Melo, and S. Rica, Phys. Rev. Lett. **79**, 4570 (1997).
[10] L.S. Tsimring and I.S. Aranson, Phys. Rev. Lett. **79**, 213 (1997).
[11] I.S. Aranson and L.S. Tsimring, Physica A **249**, 103 (1998).
[12] S.C. Venkataramani and E. Ott, Phys. Rev. Lett. **80**, 3495 (1998); Phys. Rev. E **63**, 046202 (2001).
[13] D.H. Rothman, Phys. Rev. E **57**, 1239 (1998).
[14] S.O. Jeong and H.T. Moon, Phys. Rev. E **59**, 850 (1999); S.O. Jeong, H.T. Moon, and T.W. Ko, *ibid.* **62**, 7778 (2000).
[15] J. Eggers and H. Riecke, Phys. Rev. E **59**, 4476 (1999).
[16] C. Bizon *et al.*, Phys. Rev. Lett. **80**, 57 (1998).
[17] A. Kudrolli and J.P. Gollub, Physica D **97**, 133 (1996).
[18] S. Luding *et al.*, Phys. Rev. E **49**, 1634 (1994).
[19] J.R. de Bruyn *et al.*, Phys. Rev. Lett. **81**, 1421 (1998).
[20] A. Kudrolli, B. Pier, J.P. Gollub, Physica D **123**, 99 (1998).
[21] H.-J. Pi, S.-Y. Park, J. Lee, and K.J. Lee, Phys. Rev. Lett. **84**, 5316 (2000).
[22] E. Pampaloni, S. Residori, S. Soria, and F.T. Arecchi, Phys. Rev. Lett. **78**, 1042 (1997).
[23] S.L. Judd and M. Silber, Physica D **136**, 45 (2000).
[24] J.L. Rogers *et al.*, Phys. Rev. Lett. **85**, 4281 (2000).